# Supramolecular Chemistry

# Redox-Gated Recognition of Dihydrogen Phosphate using a Ferrocene-Tethered Non-Symmetric Aryl-Triazole Pentad

Nabarupa Bhattacharjee, †a Akash Nathani, †b James B. Unzaga, b Takashi Ito, \*b Amar H. Flood\*a

## Affiliations:

- a. Department of Chemistry, Indiana University 800 E. Kirkwood Avenue, Bloomington, IN 47405, USA. \*Corresponding E-mail: aflood@indiana.edu
- b. Department of Chemistry, Kansas State University
   213 CBC Building, 1212 Mid-campus Dr North Manhattan, KS 66506
   \*Corresponding E-mail: ito@ksu.edu

#### Abstract

Anions play many roles in our environment. Consequently, the development of synthetic receptors capable of targeted anion binding is of ongoing importance. While many such receptors are known, simplified designs and measurement approaches are always beneficial. Herein, we report the synthesis of a non-symmetric aryl-triazole pentad receptor appended with a single ferrocene, its electrochemistry, and the selective binding to dihydrogen phosphate (H<sub>2</sub>PO<sub>4</sub><sup>-</sup>) anions of its oxidized form over various environmentally prevalent anions (HSO<sub>4</sub><sup>-</sup>, Cl<sup>-</sup>, NO<sub>3</sub><sup>-</sup>). The receptor was constructed using a modular architecture with simple installation of a ferrocene unit using click chemistry. Electrochemical analysis on the receptor revealed that addition of H<sub>2</sub>PO<sub>4</sub><sup>-</sup> anion led to a shift in the redox peaks of the receptor (FcP) towards more negative potentials, indicating higher anion affinity was achieved after the ferrocene was oxidized to its cationic form (FcP<sup>+</sup>). This work verifies prior studies on the efficacy of cationic charge in simpler receptor design for the creation of functional host-guest systems.

## Introduction

Anions are prevalent in the environment, serving both advantageous and deleterious roles. Ions like chloride (Cl<sup>-</sup>) is the most prevalent inorganic anion present in water bodies and it can contribute to excessive salination.<sup>1</sup> Anions like nitrate (NO<sub>3</sub><sup>-</sup>) and dihydrogen phosphate (H<sub>2</sub>PO<sub>4</sub><sup>-</sup>) are primary components of fertilizer that can run off into bodies of water causing eutrophication.<sup>2</sup>
4 Other anions play vital roles in our daily lives and biological systems.<sup>5-6</sup> Phosphates are key elements that make up DNA along with heterocyclic bases and sugars.<sup>7</sup> Phosphate and derivatives assist in energy storage and transduction as well as expression of genetic information.<sup>8-9</sup> Phosphates also play a vital role in several pharmaceutical medicines and treatments.<sup>10</sup> Bisulfate is also an essential ion required to maintain acid-base balance in our body<sup>11-12</sup> and is also used as an additive in several cleaning products and industrial raw materials.<sup>13</sup> Given these dual behaviors, it is necessary to develop efficient methods for the selective recognition of anions. To this end, supramolecular chemistry has developed many synthetic receptors capable of binding and sequestering target anions.<sup>9,14-15</sup>

A plethora of receptors have recently emerged that use only CH••••X<sup>-</sup> H-bonding. <sup>16-17</sup> These range from high affinity cages <sup>18-20</sup> and macrocycles <sup>21-23</sup> to functional foldamers <sup>24-25</sup> composed of acyclic oligomers. <sup>26</sup> Amongst these, acyclic aryl-triazole receptors incorporating ferrocene appendages <sup>27-29</sup> have been instrumental in the electrochemical detection of ions stemming from ferrocene's reversible one-electron oxidation. <sup>30-31</sup> Acyclic receptors <sup>17,32</sup> are often simpler to prepare than macrocyclic cores. <sup>33</sup> The majority of the acyclic receptors use a symmetric design with two ferrocene units appended to triazole units <sup>27-28,34</sup> or a single ferrocene centrally placed in the symmetric receptor for redox readouts. <sup>29,35</sup> Single ferrocene units have also been incorporated in creating synthetically accessible functional dyads for redox-active recognition of anions. <sup>36-38</sup>

Recently, redox-active ferrocene and fluorescent BODIPY units have been incorporated in a series of halogen and hydrogen-bonded non-symmetric acyclic anion sensors resulting in simultaneous optical and electrochemical response of anion binding. 35,39-44

In this work, we focus on designing a non-symmetric aryl triazole receptor, **FcP** (Figure 1), that incorporates a single ferrocene unit in the acyclic framework. This non-symmetric design allowed easy structural modification with ferrocene. The receptor builds upon our previous architecture by installing a neutral ferrocene in place of a cationic quinolinium. The neutral **FcP** receptor exhibits weak binding to anions such as H<sub>2</sub>PO<sub>4</sub>-, HSO<sub>4</sub>-, Cl-, and NO<sub>3</sub>-, however, the affinity towards dihydrogen phosphate anions is turned on upon electrochemical oxidation to the ferrocenium cation, **FcP**+. This study reports electrochemical investigations of anion recognition, complemented by NMR spectroscopic titrations conducted on the neutral receptor.

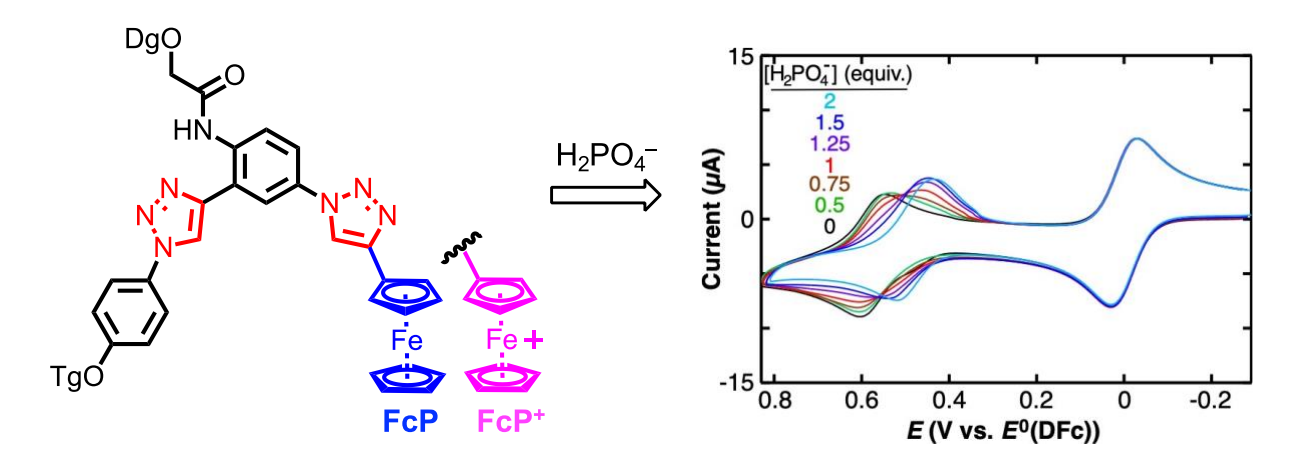


**Figure 1.** Redox-gated recognition of dihydrogen phosphate ion using ferrocene appended aryltriazole pentad, **FcP** and its oxidized form **FcP**<sup>+</sup>. (-ODg = -O(CH<sub>2</sub>CH<sub>2</sub>O)<sub>2</sub>CH<sub>3</sub>; -OTg = -O(CH<sub>2</sub>CH<sub>2</sub>O)<sub>3</sub>CH<sub>3</sub>). Electrochemical data shows the shift in ferrocene oxidation peak upon addition of dihydrogen phosphate (see below for more details).

## **Results and Discussion**

## Molecular Design and Synthesis

The pentad receptor, **FcP** (Figure 1), was designed to explore its anion binding properties. The ferrocene unit is introduced for its redox reactivity. The core of the receptor uses a prior design architecture<sup>45</sup> with two triazoles as polarized CH hydrogen bond donors for anion stabilization and two phenylene units that provide secondary hydrogen-bond contacts. An amide unit incorporated on the outer edge of the receptor forms an intramolecular hydrogen bond with the triazole to preorganize half of the receptor.<sup>26,45</sup> Use of the preorganizing unit helps reduce the number of accessible conformations leaving just two rotatable bonds. Ethylene glycol chains were used for solubility.

The receptor was prepared using a modular framework based on our prior work.<sup>45</sup> Receptor **FcP** was prepared in good yields by a click reaction between previously synthesized aryl triazole triad azide building block **1** and commercially available ethynylferrocene **2** using CuI / DIPEA catalyst system (Scheme 1 and S1).<sup>46</sup> Formation of the target receptor was confirmed using <sup>1</sup>H, <sup>13</sup>C NMR spectroscopy and high-resolution mass spectrometry.

**Scheme 1**. Preparation of **FcP**. CuI = copper iodide, DIPEA = *N*,*N*-diisopropylethylamine, THF = tetrahydrofuran, CH<sub>3</sub>CN = acetonitrile.

# Cyclic Voltammetry Studies and Anion Recognition using FcP

Cyclic voltammetry (CV) experiments were performed to test the redox-gated recognition behavior of the **FcP** receptor. Owing to the ferrocene unit attached to the aryl-triazole framework, **FcP** is expected to show redox-dependent anion recognition when subjected to electrochemical stimuli. CV data of **FcP** (0.3 mM, CH<sub>3</sub>CN) was recorded upon titrating with 0 - 2 equivalents of TBAH<sub>2</sub>PO<sub>4</sub> (Figure 2). The parent receptor, **FcP**, exhibited a reversible diffusion-controlled voltammogram with the Faradaic anodic and cathodic peaks of its ferrocene moiety at +0.61 and +0.55 V (vs.  $E^0$ (DFc)), where DFc = decamethyl ferrocene internal standard, respectively. CV measurements on **FcP** alone were carried out at different scan rates, giving the electron transfer rate constant ( $k_{s,FeP}$ ) of 0.2 cm s<sup>-1</sup> and the diffusion coefficient ( $D_{FcP}$ ) of 1.2 x 10<sup>-5</sup> cm<sup>2</sup> s<sup>-1</sup> (data not shown).<sup>47</sup>

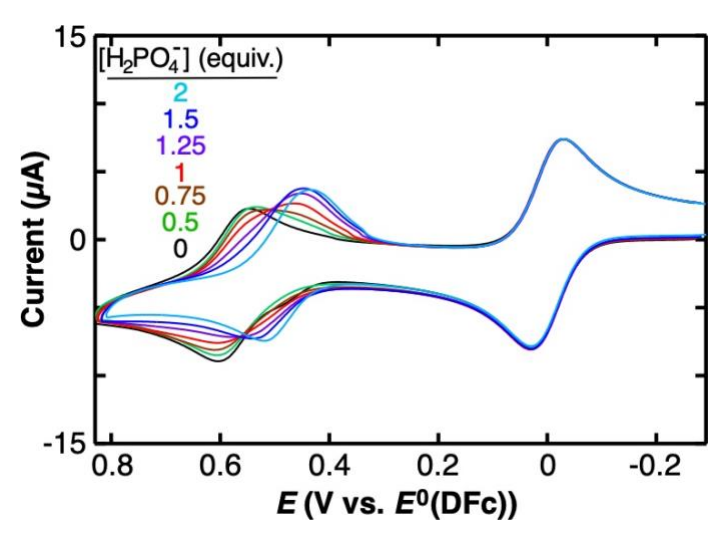


*Figure 2.* Cyclic voltammograms (0.1 V / s) of FcP (0.3 mM) measured upon sequential addition of TBAH<sub>2</sub>PO<sub>4</sub> up to 2 equivalents in 30 mM TBAPF<sub>6</sub>, CH<sub>3</sub>CN containing 0.3 mM decamethyl ferrocene as an internal standard (set to 0.0 V). Measured at a glassy carbon electrode (3 in diameter) in an argon atmosphere at room temperature (*ca.* 20°C).

Upon addition of TBAH<sub>2</sub>PO<sub>4</sub>, the Faradaic cathodic current at +0.55 V decreased and that at +0.44 V concomitantly increased up to 1.5 equivalents. Similar behavior was seen in the Faradaic anodic current of the receptor around +0.61 and +0.52 V. These observations are attributed to complexation of **FcP** with H<sub>2</sub>PO<sub>4</sub><sup>-</sup>. The observation of two separate peaks for the free and complexed **FcP** reflects the slow complexation kinetics, <sup>48</sup> as verified by digital CV simulations (*vide infra*). Negligible change in the Faradaic peak potential of the complex upon addition of 1.5 – 2 equivalents of dihydrogen phosphate implies saturation of the **FcP** receptor with 1 equivalent of the anion. The addition of TBAH<sub>2</sub>PO<sub>4</sub> had a negligible effect on the CVs of ferrocene (Figure S3), indicating that the hydrogen bonding interactions at the aryl-triazole moiety of **FcP** played a key role in the binding of H<sub>2</sub>PO<sub>4</sub><sup>-</sup>. Observation of the redox peaks for the complex at more negative potentials indicate formation of a more stable complex with the oxidized **FcP** (or **FcP**<sup>+</sup>), as shown by the following equation: <sup>48</sup>

$$\Delta E^0 = -\frac{RT}{nF} \ln \left( \frac{K_{ox}}{K_{red}} \right)$$
 (Eq. 1)

In this equation,  $\Delta E^0$  (V) is the shift of the formal potential of the receptor upon complexation,  $K_{\text{ox}}$  and  $K_{\text{red}}$  (M<sup>-1</sup>) are the binding constants of the receptor in the oxidized and reduced forms, respectively, R is the gas constant (8.314 J K<sup>-1</sup> mol<sup>-1</sup>), T is temperature (293 K), F is Faraday's constant (96,485 C mol<sup>-1</sup>), and n is the number of electrons (1 for ferrocene). Further addition of TBAH<sub>2</sub>PO<sub>4</sub>, 2–8 equivalents, led to a decrease in the Faradaic current (Figure S4), and suggests involvement of other equilibria that inhibited the electrode reaction of the receptor.

The redox-gated anion binding behavior of the **FcP** is highly selective to H<sub>2</sub>PO<sub>4</sub><sup>-</sup> over other anions examined, including HSO<sub>4</sub><sup>-</sup>, Cl<sup>-</sup>, and NO<sub>3</sub><sup>-</sup>. The addition of TBAHSO<sub>4</sub> and TBACl up to 8 equivalents led to a very small shift of the anodic and cathodic peak positions (Figure 3a and 3b). The addition of TBANO<sub>3</sub> showed a negligible change in the voltammogram (Figure 3c). The

negative shift of the Faradaic peaks for  $HSO_4^-$  and  $Cl^-$  was shown more clearly upon the addition of the larger excess of the TBA salts up to 180 equivalents (54 mM) (Figure S5ab). The oxidation of  $Cl^-$  may contribute to the visible change in CV data for TBACl, as shown by an anodic current observed at > +0.7 V (Figures 3b and S5b).

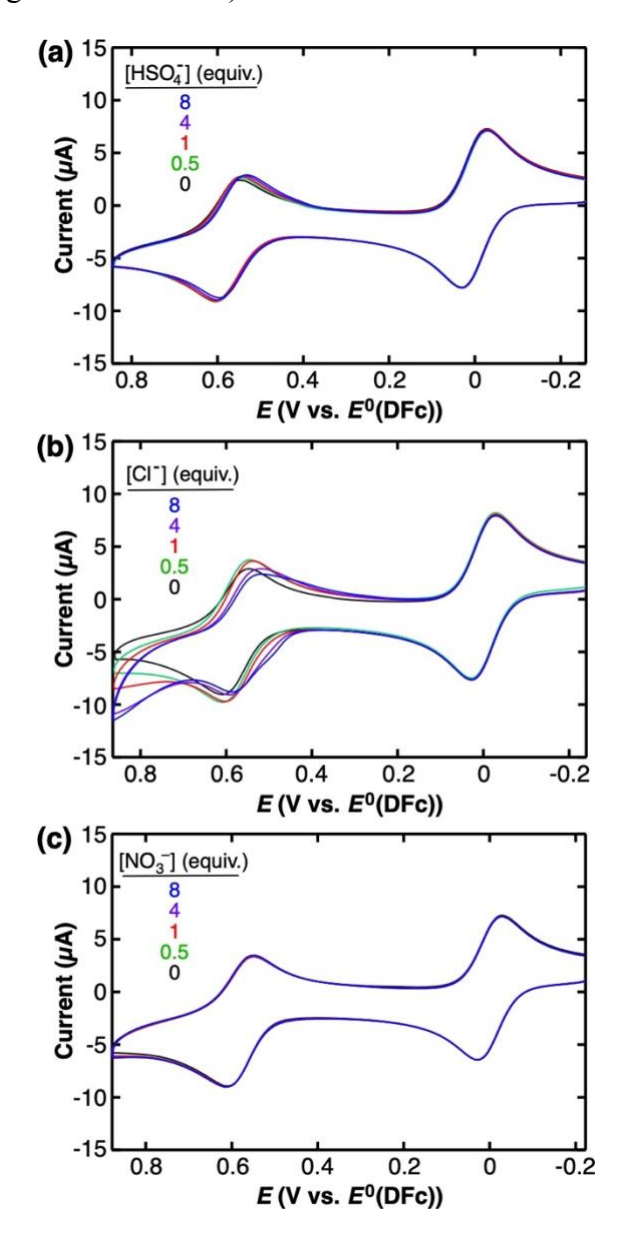
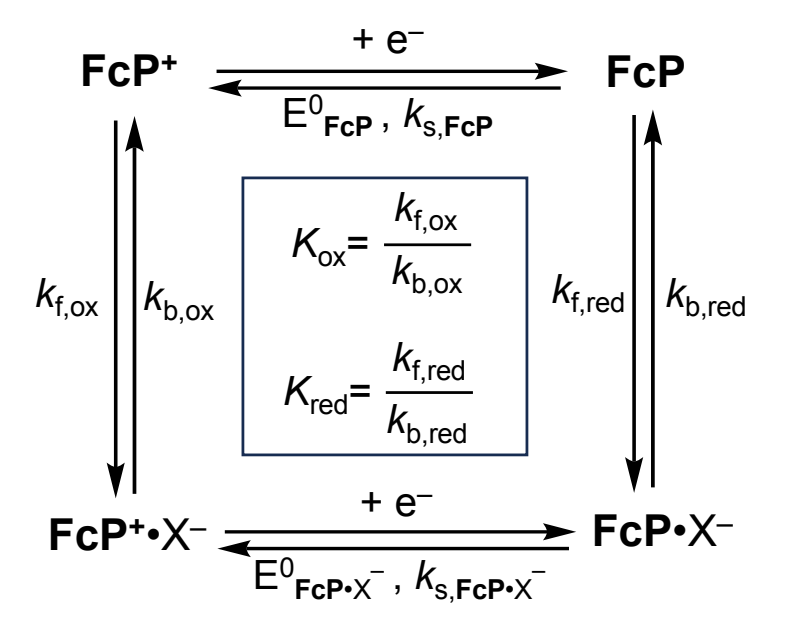


*Figure 3*. Cyclic voltammograms (0.1 V / s) of FcP (0.3 mM) measured upon sequential addition of (a) TBAHSO<sub>4</sub>, (b) TBACl, and (c) TBANO<sub>3</sub> up to 8 equivalents in 30 mM TBAPF<sub>6</sub>, CH<sub>3</sub>CN

containing 0.3 mM DFc as internal standard. Measured at a GCE (3 mm diameter) in an argon atmosphere at room temperature (*ca.* 20°C).

# Digital Simulations of the Cyclic Voltammetry Studies

Further investigations on the anion binding of FcP were investigated using digital CV simulations based on a square scheme<sup>47</sup> (Scheme 2) for H<sub>2</sub>PO<sub>4</sub><sup>-</sup> and HSO<sub>4</sub><sup>-</sup>. Simulations were carried out by assuming that the electron transfer rate constants and diffusion coefficients are unchanged upon the complexation and redox reaction of FcP. Equation 1 was used to calculate the ratio  $K_{\rm ox}/K_{\rm red}$  from the experimental  $\Delta E^0$  data obtained at 2 and 180 equivalents for H<sub>2</sub>PO<sub>4</sub><sup>-</sup> and HSO<sub>4</sub><sup>-</sup>, respectively. All the parameters employed for the digital simulations are summarized in Table S1. Figure S6ab shows the experimental and simulated CV data, respectively, for H<sub>2</sub>PO<sub>4</sub><sup>-</sup> up to 1.5 equivalents. As summarized in Table S1b, the experimental data could be qualitatively replicated using  $K_{\text{red}} = 500 \text{ M}^{-1} (15.4 \text{ kJ mol}^{-1})$  and  $K_{\text{ox}} = 29,600 \text{ M}^{-1} (25.5 \text{ kJ mol}^{-1})$ . The estimated  $K_{\text{red}}$  value was kept lower, assuming the weak binding of the reduced form of the receptor with the dihydrogen phosphate anion. The large binding affinity,  $K_{ox}$ , for the oxidized receptor indicates the significant contribution from electrostatic attraction. The complexation rate of the oxidized receptor was much lower ( $k_{\rm f,ox} = 100 \, {\rm M}^{-1} \, {\rm s}^{-1}$ ) than that of the reduced form ( $k_{\rm f,red} = 500,000 \, {\rm M}^{-1} \, {\rm s}^{-1}$ ) <sup>1</sup>). The experimental data for  $HSO_4^-$  could be replicated (Figure S7ab) with the much smaller  $K_{red}$ and  $K_{\rm ox}$  values ~ 30 and 400 M<sup>-1</sup>, respectively; (Table S1), as expected from the small changes in the CVs upon addition of the anion (Figures 3a and S5a).



**Scheme 2**. Square scheme used for the digital CV simulations.

# Anion Binding to the Neutral FcP Receptor using <sup>1</sup>H NMR Spectroscopy

Receptor **FcP** was titrated with the suite of four anions H<sub>2</sub>PO<sub>4</sub><sup>-</sup>, Cl<sup>-</sup>, NO<sub>3</sub><sup>-</sup>, and HSO<sub>4</sub><sup>-</sup> in acetonitrile solutions under conditions that mimic those used in electrochemistry experiments (Figure 4, S12, S15, S16). The species formed upon complexation of the anions with the neutral (reduced) form of the receptor were characterized using <sup>1</sup>H NMR titrations.

Upon addition of 0 to 300 equivalents of TBAH<sub>2</sub>PO<sub>4</sub> to **FcP** (0.3 mM, CD<sub>3</sub>CN) containing 30 mM of TBAPF<sub>6</sub>, we observe the largest migration of triazole protons (H<sup>c</sup>) on order 1.1 ppm. These shifts are followed by triazole H<sup>e</sup> by 1 ppm and the central phenylene proton H<sup>d</sup> by 0.5 ppm (Figure 4). These shifts are assigned to formation of a 1:1 **FcP**•H<sub>2</sub>PO<sub>4</sub><sup>-</sup> complex. The need for excess anion is indicative of formation of a weak binding 1:1 host-guest complex. The downfield shifts for the two triazoles and central phenylene protons indicate CH•••H<sub>2</sub>PO<sub>4</sub><sup>-</sup> hydrogen bonds being formed in the central cavity. For the cyclopentadienyl ring of the ferrocene unit bonded to the triazole, the proton closer to the central cavity, H<sup>i</sup>, shifts more (0.2 ppm downfield) than the

one facing away from the cavity (H<sup>'</sup>, 0.03 ppm upfield). The protons in the lower cyclopentadienyl ring of the ferrocene unit show little to no shifts upon addition of the anion. The magnitude of the shifts correlates qualitatively with the strength of the H-bonding contacts. The greatest shifts are observed for the triazole protons suggesting they form stronger hydrogen bonds. All other protons shift to a much lesser degree. Collectively, these NMR signatures support the formation of a weak 1:1 complex with the H<sub>2</sub>PO<sub>4</sub><sup>-</sup> ion binding to the central pocket in the neutral form of the receptor. Similar changes were seen (Figure S11) when titrations were conducted in absence of externally added TBAPF<sub>6</sub>.

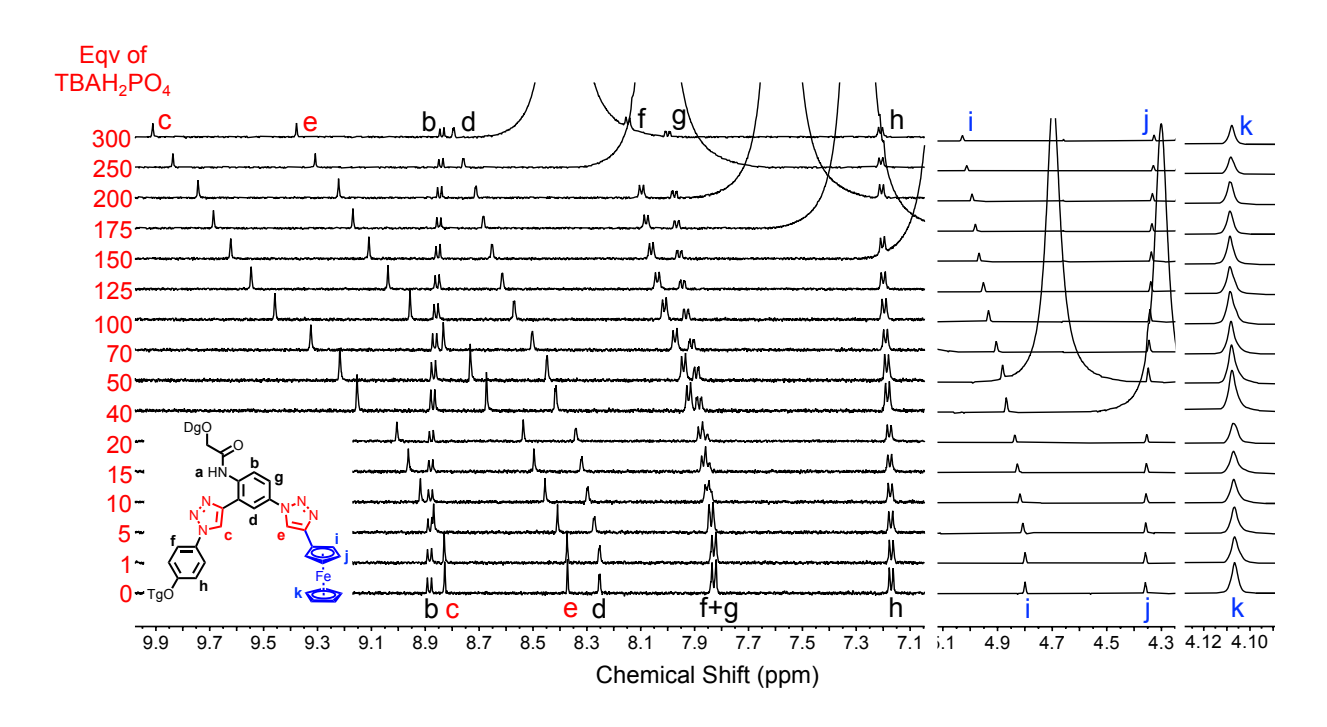


*Figure 4.* <sup>1</sup>H NMR titration of FcP (0.3 mM, CD<sub>3</sub>CN, 30 mM TBAPF<sub>6</sub>, 298 K) with TBAH<sub>2</sub>PO<sub>4</sub> (0 to 300 equivalents).<sup>49</sup>

Titrations were conducted using similar procedures with other ions (Cl<sup>-</sup>, NO<sub>3</sub><sup>-</sup>, HSO<sub>4</sub><sup>-</sup>) under the same conditions employed for H<sub>2</sub>PO<sub>4</sub><sup>-</sup>. The chemical shift variations of the representative triazole proton (H<sup>c</sup>) were monitored. Notably, the observed chemical shift changes ( $\Delta\delta$ ) were 1.7, 0.3 and 0.2 ppm for Cl<sup>-</sup>, NO<sub>3</sub><sup>-</sup> and HSO<sub>4</sub><sup>-</sup> respectively, in contrast to 1.1 ppm for

H<sub>2</sub>PO<sub>4</sub><sup>-</sup> (Table S2). Analysis of the binding behaviors of the neutral form of the receptor reveals weak interactions for all anions, as evident from the subtle binding curvature observed in the titration binding plots (Figure 5). Furthermore, saturation was not reached even with the addition of 300 equivalents of the salts for all the anions. For HSO<sub>4</sub><sup>-</sup>, titration was performed with addition of the salt only up to 200 equivalents due to significant broadening of the peaks (Figure S16). Peak broadening was observed beyond 100 equivalents of the salt. For the **FcP** receptor, it is interesting to note a slightly steeper binding curvature (affinity) of the neutral receptor for Cl<sup>-</sup> (Figure 5). This could be attributed to a reduced competition from ion pairing of the salt (log  $K_{TBACl} = 0.73$ ),<sup>50</sup> as opposed to the phosphate salt (log  $K_{TBAH2PO4} = 1.90$ ) in acetonitrile (Figure S18).

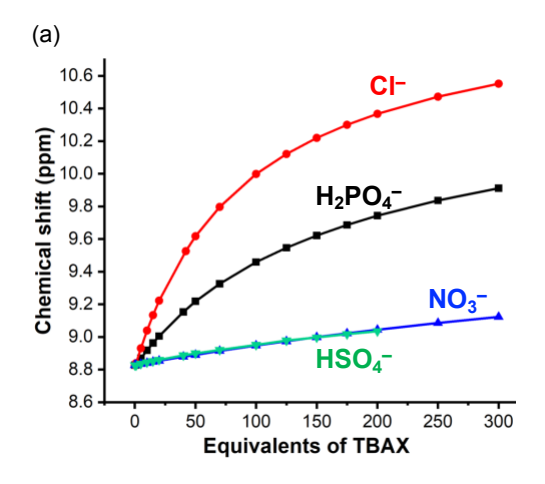


*Figure 5*. Changes in chemical shift of triazole proton H<sup>c</sup> upon addition of TBAX salts (0 to 300 equivalents) to FcP (0.3 mM, CD<sub>3</sub>CN).

Apparent binding constants were first determined using Bindfit<sup>51</sup> for Cl<sup>-</sup> and H<sub>2</sub>PO<sub>4</sub><sup>-</sup> (Figures S9 and S13). The apparent binding constants were determined to be  $\log K_{\rm H2PO4} = 1.30$  and  $\log K_{\rm Cl} = 1.56$ . This software cannot currently include the additional equilibrium needed to account for ion pairing. The effect of solvent on ion pairing as well as on the binding affinity of the receptor have been extensively studied<sup>45,50,52</sup> but is outside the scope of the current work. Thus, we assume that the actual binding affinities are greater depending on the degree of ion pairing

under the conditions examined. We tested this hypothesis using HypNMR<sup>53</sup> (Figures S10 and S14) which allows for the inclusion of multiple equilibria (Eq. 2-4, *vide infra*). In this global fitting, we used the 1:1 binding equilibrium for dihydrogen phosphate and chloride with **FcP** (Eq. 2). The binding of PF<sub>6</sub><sup>-</sup> binding with **FcP** was negligible and could reasonably be ignored (Figure S17). We included the ion pairing reactions for TBAPF<sub>6</sub> (Eq. 3) and either TBAH<sub>2</sub>PO<sub>4</sub> or TBACl (Eq. 4). Consistent with our expectation, we found  $\log K_{\rm H2PO4} = 1.81$  (Table 1). With the lower degree of ion pairing for TBACl, there was no change in the binding affinity (Table 1). A plot of the speciation shows the influence of ion pairing in case of the phosphate titration (Figure S19).

$$\mathbf{FcP} + \mathbf{X}^{-} \Longrightarrow \mathbf{FcP} \cdot \mathbf{X}^{-}$$
 (Eq. 2)  
 $\mathbf{TBA}^{+} + \mathbf{PF6}^{-} \Longrightarrow \mathbf{TBA} \cdot \mathbf{PF6}$  (Eq. 3)

Binding of the nitrate and bisulfate anions was too weak to allow a global fit using the coupled set of equilibria, Equations 2-4. Hence, we simplified the system without considering any ion pairing interactions (Eq. 3-4) to estimate the apparent binding constant. A low equilibrium constant was obtained as is consistent with our expectation (Table 1). Speciation curves reflecting the apparent (without ion-pairing) and the complete (with ion pairing) binding constants of the neutral receptor are shown in Figure S20a and S20b.

(Eq. 4)

Table 1. Binding data for FcP

 $TBA^+ + X^- \Longrightarrow TBA \cdot X$ 

Anion	$\log K_{\text{neutral}}(1:1)$	$K_{\text{neutral}}$ (1:1) / $M^{-1}$	log K <sub>apparent</sub> (1:1) / M <sup>-1</sup>
H <sub>2</sub> PO <sub>4</sub> <sup>-</sup>	$a 1.81 \pm 0.03$	65	
			$^{b}$ 1.30 ± 0.01
Cl-	$a 1.56 \pm 0.01$	36	
			$^{b}$ 1.56 ± 0.01

$NO_3^-$	4	$^{b}$ 0.60 $\pm$ 0.03
HSO <sub>4</sub> <sup>-</sup>	10	$^{b}$ 0.98 ± 0.05

- a. Measured by independent <sup>1</sup>H NMR titration experiments (0.3 mM FcP and 30 mM TBAPF<sub>6</sub> in CD<sub>3</sub>CN) and analyzed using HypNMR. Ion pairing was accounted for in the fitting.
- b. Binding constants were estimated using solely a 1:1 binding reaction between the anion and **FcP** and ignoring any ion pairing interactions from the salts. Analysis completed using Bindfit.

#### Control studies in acetonitrile

To ensure the absence of any interactions between the background PF<sub>6</sub><sup>-</sup> ion and the H<sub>2</sub>PO<sub>4</sub><sup>-</sup> salt, a separate titration experiment was conducted. In this experiment, a solution of TBAH<sub>2</sub>PO<sub>4</sub> was titrated into a 1 mM solution of TBAPF<sub>6</sub> in CD<sub>3</sub>CN. No noticeable shifts were observed in the <sup>19</sup>F signals of the PF<sub>6</sub><sup>-</sup> ion during this titration, indicating lack of any secondary interactions between the dihydrogen phosphate ion and PF<sub>6</sub><sup>-</sup> that might influence the results of the electrochemistry experiments (Figure 6).

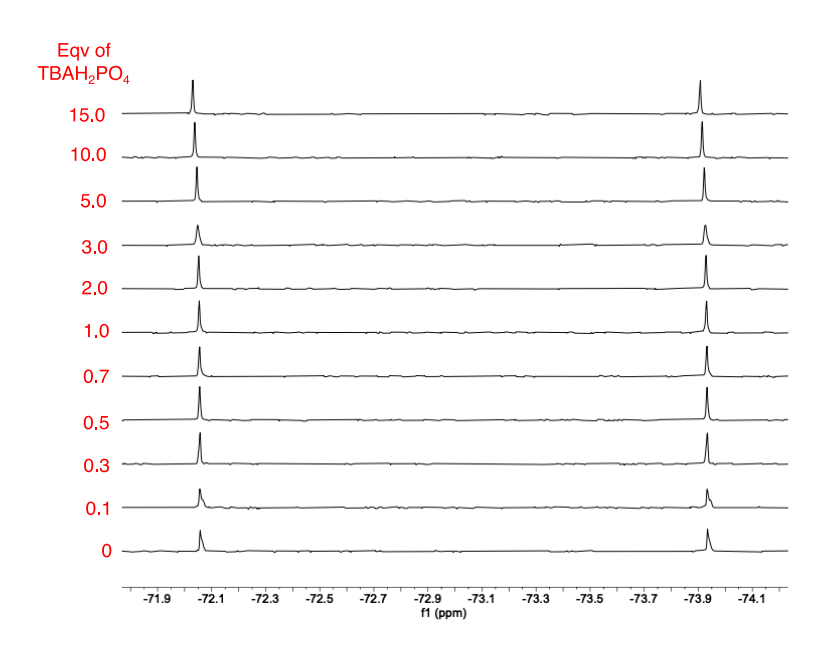


*Figure 6*. <sup>19</sup>F NMR titration of TBAPF<sub>6</sub> (1 mM, CD<sub>3</sub>CN, 298 K) with TBAH<sub>2</sub>PO<sub>4</sub> (0 to 15 equivalents).

A separate titration of the neutral **FcP** with TBAPF<sub>6</sub> (Figure S17) was performed to ensure that the PF<sub>6</sub><sup>-</sup> anion does not compete in binding with the target anions. Under similar conditions (0.3 mM, CD<sub>3</sub>CN), none of the protons showed any noticeable shifts, thereby confirming no association of the PF<sub>6</sub><sup>-</sup> ion with the receptor.

#### Molecular Modelling

Computational calculations were performed to optimize the geometry of the neutral versions of the empty receptor as well as the chloride and dihydrogen phosphate complexes (Figures S21-S23). Using DFT (B3LYP/6-31G\*) level of theory, geometries of anion bound complexes were evaluated. To prevent distortions in the geometry of the ferrocene unit during optimization calculations, the ferrocene atoms were constrained to remain fixed. This is evident in the observed fixed positions in the calculated structures (Figure 7). This constraint still allowed rotation around the bond connecting the ferrocene to the receptor body. Both anions are observed to sit within the central cavity of the receptor. As expected, all the protons establish shorter hydrogen bonds with the larger dihydrogen phosphate anion compared to Cl<sup>-</sup> (Table 2). We observe the cyclopentadienyl ring that is coplanar with the body of the receptor to form shorter hydrogen bonds than the lower one (Table 2).

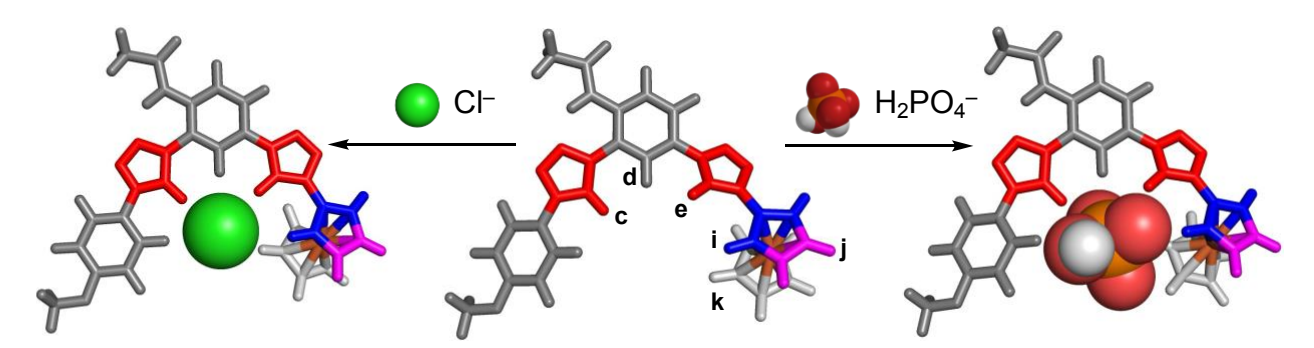


*Figure 7*. Molecular structures of the **FcP** receptor and its complexes. Structure was simplified by truncating side chains to methyl units. Ferrocene protons are color coded for clarity:  $H^i$  (blue, 2 protons), proton  $H^j$  (magenta, 2 protons) and  $H^k$  (white, 5 protons).

Table 2. Hydrogen bond distances for FcP calculated from the optimized geometries.

H <sub>2</sub> PO <sub>4</sub> <sup>-</sup> (Å)	Cl <sup>-</sup> (Å)
2.0 (CH•••O)	2.3
2.3 (CH•••O)	2.8
2.3 (CH•••O⁻)	2.5
2.2 (CH•••O⁻)	3.4
2.9 (CH•••O)	2.9
	2.0 (CH•••O) 2.3 (CH•••O) 2.3 (CH•••O <sup>-</sup> ) 2.2 (CH•••O <sup>-</sup> )

## **Conclusions**

We developed a non-symmetric ferrocene-integrated receptor that displays selective recognition of dihydrogen phosphate over chloride, nitrate, and bisulfate in its singly oxidized form. In the neutral state, the receptor exhibits notably weak binding affinity towards all four anions. Use of CV to effect electrochemical oxidation to its cationic form of the receptor shows a negative peak shift exclusively for dihydrogen phosphate ions indicating the affinity for this anion increases by a factor of 500, increasing from ~60 to ~30,000 M<sup>-1</sup>. This study emphasizes previous research results utilizing cationic receptors showing how positive charges enhance affinities, and influences selectivity.

# **Experimental Section**

The experimental details outlined in the Supporting Information include synthesis, NMR and electrochemistry-based titrations, ESI-MS, and computational chemistry.

## Acknowledgements

We acknowledge support from the NSF (CHE-2305013). J.B.U. was supported by NSF REU grant number CHE-1852182. We acknowledge NMR support from NSF MRI CHE-1920026. The prodigy probe was partially funded by Indiana Clinical and Translational Sciences Institute. In addition, we thank Dr. Li Sun (Pine Research Instrumentation) for his help with the digital CV simulations.

# **Keywords**

Anions; Recognition; Ferrocene; Triazoles.

#### References

- 1. S. S. Kaushal; P. M. Groffman; G. E. Likens; K. T. Belt; W. P. Stack; V. R. Kelly; L. E. Band; G. T. Fisher. *Proc. Natl. Acad. Sci. U.S.A.* **2005**, *102*, 13517-13520.
- 2. D. L. Correll. J. Environ. Qual. 1998, 27, 261-266.
- 3. B. Moss. Chem. Ind. 1996, 407-411.
- 4. S. R. Carpenter; N. F. Caraco; D. L. Correll; R. W. Howarth; A. N. Sharpley; V. H. Smith. *Ecol Appl* **1998**, *8*, 559-568.
- 5. R. Dutzler; E. B. Campbell; M. Cadene; B. T. Chait; R. MacKinnon. *Nature* **2002**, *415*, 287-294.
- 6. T. Sato; H. Konno; Y. Tanaka; T. Kataoka; K. Nagai; H. H. Wasserman; S. Ohkuma. *J. Biol. Chem.* **1998**, *273*, 21455-21462.
- 7. R. L. P. Adams; J. T. Knowler; D. P. Leader. *The biochemistry of the nucleic acids*; Springer Science & Business Media, 2013.
- 8. J. R. Knowles. Annual Review of Biochemistry 1980, 49, 877-919.
- 9. J. L. Sessler; P. Gale; W.-S. Cho. *Anion Receptor Chemistry*; The Royal Society of Chemistry, 2006. DOI: 10.1039/9781847552471.
- 10. S. M. Moe. *Prim. Care* **2008**, *35*, 215-237.
- 11. J. W. Pflugrath; F. A. Quiocho. Nature 1985, 314, 257-260.
- 12. B. Sen; M. Mukherjee; S. Pal; S. Sen; P. Chattopadhyay. RSC Adv. 2015, 5, 50532-50539.
- 13. A. Huss; R. Cochrane; C. Jones; G. G. Atungulu. Chapter 5 Physical and Chemical Methods for the Reduction of Biological Hazards in Animal Feeds. In *Food and Feed Safety Systems and Analysis*, Ricke, S. C., Atungulu, G. G., Rainwater, C. E., Park, S. H. Eds.; Academic Press, 2018; pp 83-95.
- 14. M. Wenzel; J. R. Hiscock; P. A. Gale. Chem. Soc. Rev. 2012, 41, 480-520.
- 15. L. K. Macreadie; A. M. Gilchrist; D. A. McNaughton; W. G. Ryder; M. Fares; P. A. Gale. *Chem* **2022**, *8*, 46-118.
- 16. Y. Hua; A. H. Flood. Chem. Soc. Rev. 2010, 39, 1262-1271.
- 17. K. P. McDonald; R. O. Ramabhadran; S. Lee; K. Raghavachari; A. H. Flood. *Org. Lett.* **2011**, *13*, 6260-6263.

- 18. Y. Liu; W. Zhao; C.-H. Chen; A. H. Flood. Science 2019, 365, 159-161.
- 19. J. Samanta; M. Tang; M. Zhang; R. P. Hughes; R. J. Staples; C. Ke. *J. Am. Chem. Soc.* **2023**, *145*, 21723-21728.
- 20. Y. Chen; G. Wu; L. Chen; L. Tong; Y. Lei; L. Shen; T. Jiao; H. Li. *Org. Lett.* **2020**, *22*, 4878-4882.
- 21. Y. Li; A. H. Flood. J. Am. Chem. Soc. 2008, 130, 12111-12122.
- 22. J. L. Sessler; J. Cai; H.-Y. Gong; X. Yang; J. F. Arambula; B. P. Hay. *J. Am. Chem. Soc.* **2010**, *132*, 14058-14060.
- 23. S. Lee; C.-H. Chen; A. H. Flood. Nat. Chem. 2013, 5, 704-710.
- 24. Y. Hua; A. H. Flood. J. Am. Chem. Soc. 2010, 132, 12838-12840.
- 25. Y. Liu; F. C. Parks; E. G. Sheetz; C.-H. Chen; A. H. Flood. *J. Am. Chem. Soc.* **2021**, *143*, 3191-3204.
- 26. S. Lee; Y. Hua; H. Park; A. H. Flood. Org. Lett. 2010, 12, 2100-2102.
- 27. Q.-Y. Cao; T. Pradhan; S. Kim; J. S. Kim. Org. Lett. 2011, 13, 4386-4389.
- 28. Q.-Y. Cao; T. Pradhan; M. H. Lee; D. H. Choi; J. S. Kim. *Tetrahedron Lett.* **2012**, *53*, 4917-4920.
- 29. J. Y. C. Lim; M. J. Cunningham; J. J. Davis; P. D. Beer. *Chem. Commun.* **2015**, *51*, 14640-14643.
- 30. P. D. Beer; Z. Chen; A. J. Goulden; A. Graydon; S. E. Stokes; T. Wear. *J. Chem. Soc., Chem. Commun.* **1993**, 1834-1836.
- 31. L. Fabbrizzi. ChemTexts 2020, 6, 22.
- 32. J. Shang; W. Zhao; X. Li; Y. Wang; H. Jiang. Chem. Commun. 2016, 52, 4505-4508.
- 33. Y. Hua; R. O. Ramabhadran; J. A. Karty; K. Raghavachari; A. H. Flood. *Chem. Commun.* **2011**, *47*, 5979-5981.
- 34. C.-T. Li; Q.-Y. Cao; J.-J. Li; Z.-W. Wang; B.-N. Dai. *Inorganica Chim. Acta* **2016**, *449*, 31-37.
- 35. J. Y. C. Lim; P. D. Beer. Eur. J. Inorg. Chem. 2017, 2017, 220-224.
- 36. T. Romero; A. Caballero; A. Tárraga; P. Molina. Org. Lett. 2009, 11, 3466-3469.
- 37. Q.-Y. Cao; T. Pradhan; M. H. Lee; K. No; J. S. Kim. Analyst 2012, 137, 4454-4457.
- 38. Q.-Y. Cao; Y.-M. Han; P.-S. Yao; W.-F. Fu; Y. Xie; J.-H. Liu. *Tetrahedron Lett.* **2014**, *55*, 248-251.
- 39. A. J. Taylor; R. Hein; S. C. Patrick; J. J. Davis; P. D. Beer. *Angew. Chem. Int. Ed. n/a*, e202315959.
- 40. S. Madhu; M. Ravikanth. *Inorganic Chemistry* **2014**, *53*, 1646-1653.
- 41. P. Ashokkumar; H. Weißhoff; W. Kraus; K. Rurack. *Angew. Chem. Int. Ed.* **2014**, *53*, 2225-2229
- 42. Y. Cheong Tse; R. Hein; E. J. Mitchell; Z. Zhang; P. D. Beer. *Chem. Eur. J.* **2021**, *27*, 14550-14559.
- 43. F. Zapata; A. Caballero; P. Molina. Eur. J. Inorg. Chem. 2017, 2017, 237-241.
- 44. J. Y. C. Lim; I. Marques; L. Ferreira; V. Félix; P. D. Beer. *Chem. Commun.* **2016**, *52*, 5527-5530.
- 45. N. Bhattacharjee; X. Gao; A. Nathani; J. R. Dobscha; M. Pink; T. Ito; A. H. Flood. *Chem. Eur. J.* **2023**, *29*, e202302339.
- 46. V. S. Shetti; M. Ravikanth. Eur. J. Org. Chem. 2010, 2010, 494-508.
- 47. A. J. Bard; L. R. Faulkner; H. S. White. *Electrochemical Methods: Fundamentals and Applications*; Wiley, 2022.

- 48. R. Hein; P. D. Beer; J. J. Davis. Chem. Rev. 2020, 120, 1888-1935.
- 49. We reason that the marked shift in the water signal occurs upon interaction of water with the OH proton of the dihydrogen phosphate anion. With an increasing concentration of the unbound anion, the residual water from the solvent and the salt interacts, resulting in a large downfield shift of the water signal.
- 50. Y. Liu; A. Sengupta; K. Raghavachari; A. H. Flood. Chem 2017, 3, 411-427.
- 51. http://supramolecular.org.
- 52. Y. Hua; R. O. Ramabhadran; E. O. Uduehi; J. A. Karty; K. Raghavachari; A. H. Flood. *Chem. Eur. J.* **2011**, *17*, 312-321.
- 53. C. Frassineti; S. Ghelli; P. Gans; A. Sabatini; M. S. Moruzzi; A. Vacca. *Anal. Biochem.* **1995**, *231*, 374-382.